INTRA–KERNEL MOISTURE RESPONSES OF RICE TO DRYING AND TEMPERING TREATMENTS BY FINITE ELEMENT SIMULATION

W. Yang, C.–C. Jia, T. J. Siebenmorgen, T. A. Howell, A. G. Cnossen

ABSTRACT. *Moisture content patterns inside rice kernels are important in understanding rice fissure formation, especially when glass transition effects are considered. Unsteady and non–linear partial differential equations were employed to describe two–dimensional temperature and moisture distributions within a single rice kernel during drying and tempering processes. Moisture content gradients (MCGs) inside the kernel were examined. Results showed that the maximum MCG (MMCG) appeared in the direction of the short axis. During the tempering process, moisture content on the kernel surface had a much faster and greater change than that at the kernel center. The intra–kernel MCG decreased considerably during the first 40 min of tempering, after which it decreased slowly to approach zero. A duration of about 40 min of tempering at 60°C helped eliminate about 90% of the MCGs created inside the rice kernel during drying, and this simulation result correlated favorably with the published tempering data in the literature. The findings from this study provided useful information for determining optimal drying and tempering conditions of rice to enhance its milling quality.*

Keywords. *Rice, Finite element method, Numerical simulation, Moisture content gradient, Drying, Tempering.*

A study of intra–kernel, instead of grain bulk, moisture content responses to drying and tempering treatments can help us better understand the factors affecting the drying and tempering processes. This is because it is the individual kernels inside a bulk that interact with the drying medium, despite the fact that grains are usually dried in bulk. The individual kernel quality gives an index of the overall grain quality.

High–temperature drying can increase the drying rate of rice, but it is also associated with an increased potential of fissuring. Because of this, rice is often dried at a low temperature (e.g., 40°C or lower) in practice to maintain a higher head rice yield, although doing so takes an extended length of time to dry rice from a harvest moisture content of 16% to 21% wet basis (w.b.) to a moisture content safe for storage (around 13% w.b.). Previous research on rice drying and tempering by Cnossen et al. (1999) has shown that high drying temperatures and high moisture removal rates per drying pass could be used without reducing milling quality, if tempering at a temperature above the glass transition temperature (T_g) is performed between drying passes. High tempering temperatures have been shown to reduce the length of time required to temper grain without reducing its milling quality (Wasserman et al., 1964; Steffe and Singh, 1980b).

A considerable number of theoretical and experimental studies has been conducted to describe the drying process of grains. Luikov (1966) developed a mathematical model for describing the drying of porous media. Some researchers applied this model to grain drying. Husain et al. (1972, 1973) concluded that consideration of the coupling effects of temperature and moisture in the analysis of grain drying is not required for engineering practice. Haghighi and Segerlind (1988), Haghighi et al. (1990), Irudayaraj et al. (1992), and Jia et al. (2000) combined Luikov's model and considered the effects of thermal behavior of grain and internal temperature and moisture gradients, which increased the drying simulation accuracy. Sokhansanj and Bruce (1987) proposed a model for grain drying which assumed that the liquid form of moisture diffused to the outer boundary of the kernel and evaporated on the surface of the grain. This assumption was supported by wheat drying experiments conducted by Fortes et al. (1981a, 1981b). However, some assumptions, such as the constant diffusion coefficient and material properties for simplifying calculations, could affect the simulation accuracy. In the meantime, the effect of possible moisture evaporation inside the grain kernel is also worthy of consideration. Furthermore, few people paid attention to MCG patterns during drying and tempering, as well as their effect on the quality of final products.

The objectives of this study were to:

1. Apply the finite element method to predict intra–kernel moisture content distribution during drying and tempering processes of rice.
2. Examine the relations between MCGs and head rice yield trends during drying and tempering processes.

Article was submitted for review in September 2001; approved for publication by the Food & Process Engineering Institute of ASAE in April 2002. Presented at the 2000 ASAE Annual Meeting as Paper No. 006003.

The authors are **Wade Yang**, **ASAE Member Engineer**, Research Assistant Professor; **Canchun Jia**, Research Associate; **Terry J. Siebenmorgen**, **ASAE Member Engineer**, Professor; **Terry A. Howell**, **ASAE Member Engineer**, Research Assistant Professor; and **Auke G. Cnossen**, Research Specialist; Department of Food Science, University of Arkansas, Fayetteville, Arkansas **Corresponding author**: Wade Yang, Department of Food Science, University of Arkansas, 2650 N. Young Ave., Fayetteville, AR 72704; phone: 479–575–4678; fax: 479–575–6936; e–mail: wyang@uark.edu.

Materials and Methods

Drying Model

It is generally assumed that moisture flow within a grain kernel takes place by diffusion. The surface of the kernel exchanges heat with ambient by convection, while the internal part of the kernel is heated by conduction. Assuming that moisture diffuses to the outer boundary of the kernel in both liquid and vapor forms and that evaporation takes place both on the surface and inside the kernel, the heat and moisture transfer equations can be written as follows for a cylindrical coordinate system:

$$\frac{\partial M}{\partial t} = D\left(\frac{\partial^2 M}{\partial r^2}\right) + D\left(\frac{1}{r}\frac{\partial M}{\partial r}\right) + D\left(\frac{\partial^2 M}{\partial z^2}\right) \quad (1)$$

$$\rho_g c_g \frac{\partial T}{\partial t} = k\left(\frac{\partial^2 T}{\partial r^2}\right) + k\left(\frac{1}{r}\frac{\partial T}{\partial r}\right) + k\left(\frac{\partial^2 T}{\partial z^2}\right) + \rho_g Q_{fg}\frac{1}{1+M}\frac{\partial M}{\partial t} \quad (2)$$

where the last term in equation 2 reflects moisture evaporation. The corresponding boundary and initial conditions for equations 1 and 2 during drying are:

$$-D\frac{\partial M}{\partial n} = h_m(M - M_e) \quad (3)$$

$$-k\frac{\partial T}{\partial n} = h_t(T - T_a) + \rho_g\left[Q_{fg} + c_V(T_a - T)\right]\frac{V}{A(1+M)}\frac{\partial M}{\partial t} \quad (4)$$

$$t = 0, \quad M = M_0, \quad T = T_0 \quad (5)$$

where D is an effective overall moisture diffusivity accountable to both liquid and vapor diffusion.

Adiabatic Tempering Model

In a tempering process, grain is maintained in an insulated, adiabatic environment immediately after drying so that moisture inside grain kernels can equalize between the center and surface of the kernel at a constant temperature. In practice, however, the temperature usually decreases gradually due to imperfect insulation. In this study, only adiabatic tempering at a temperature equal to that of the drying air was considered.

During tempering, only diffusion phenomena exist, and the average temperature and moisture content of rice are basically kept constant (Steffe and Singh, 1980b; Gustafson et al., 1983; Jia et al., 1996). The boundary conditions are:

$$\frac{\partial M}{\partial n} = 0 \quad (6)$$

$$\frac{\partial T}{\partial n} = 0 \quad (7)$$

At the onset of tempering, moisture and temperature profiles inside the kernel are equal to those at the end of drying, i.e.:

$$t = 0$$
$$M(r,z) = M(r,z)_{dryingend}$$
$$T(r,z) = T(r,z)_{dryingend} \quad (8)$$

Finite Element Analysis

In this study, a rough rice kernel was assumed to be a 3–layer body containing hull, bran, and endosperm (fig. 1), and the dimensions of a rice kernel were the average values of 1000 kernels measured with an image analyzer (Satake, Taito–ku, Tokyo) (Bautista et al., 2000). The rice kernel was divided into triangular elements. A two–dimensional axisymmetric finite element grid of a quarter section of a single rough rice kernel in the cylindrical co–ordinate is shown in figure 1. The mesh was automatically optimized upon creation by the PDE module of Matlab (The Math Works, Inc., Natick, Mass.). The element equations were developed from the above governing differential equations by transforming them using the Galerkin's weighed residual methods. Green's formula was used to simplify the variation equations of the whole area. Finally, equations 1 and 2 was expressed in a general matrix form:

$$[C]\begin{Bmatrix}\dot{M}\\ \dot{T}\end{Bmatrix} + [K]\begin{Bmatrix}M\\ T\end{Bmatrix} - \begin{Bmatrix}F_M\\ F_T\end{Bmatrix} = 0 \quad (9)$$

The backward difference method was used to approximate $\{T\}$ and $\{M\}$ in the i time step; therefore, equation 9 became:

$$\left([C] + \Delta t[K]\right)\begin{Bmatrix}M\\ T\end{Bmatrix}_{i+1} = [C]\begin{Bmatrix}M\\ T\end{Bmatrix}_i + \Delta t\begin{Bmatrix}F_M\\ F_T\end{Bmatrix}_i \quad (10)$$

A simulation program using the finite element method, based on the above analyses, was developed using Matlab. The program first solves $\{M\}_{i+1}$ in equation 10, and then substitutes it into equation 10 to obtain $\{T\}_{i+1}$. Because the

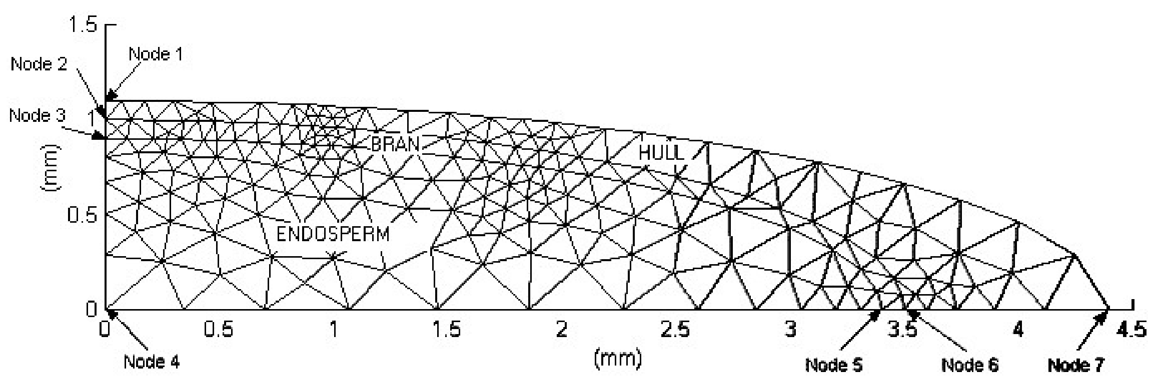

Figure 1. Finite element mesh of a long–grain (cv. Cypress) rice kernel (1/4 section).

Table 1. The parameters, formulas, and simulation conditions used in this study.

Parameter	Value or Formulation[a]	References
c_a	1013	Brooker et al. (1992)
c_g	For endosperm: $1180 + 3766 \times M_{ave}$ For bran: $0.125/[1/(1201 + 3807 \times M_{ave}) - 0.875/c_{endosperm}]$ For hull: $0.2/[1/(1109 + 4477 \times M_{ave}) - 0.1/c_{bran} - 0.7/c_{endosperm}]$	Lague and Jenkins (1991)
c_v	1880	Brooker et al. (1992)
D	$c_1 \times \exp[-c_2/(T_{ave} + 273)]$ For hull: $c_1 = 4.84 \times 10^2$; $c_2 = 7380.8$ For bran: $c_1 = 7.97 \times 10^{-1}$; $c_2 = 5110$ For endosperm: $c_1 = 2.57 \times 10^{-3}$; $c_2 = 2880$	Steffe and Singh (1980a)
h_m	$0.01959 + 0.08073 \times u^{0.553}$	Lague and Jenkins (1991)
h_t	$16.09 + 65.87 \times u^{0.53}$	Lague and Jenkins (1991)
Q_{fg}	$1000 \times (1 + 2.07 \times e^{-21.74 \times M_{ave}}) \times (2502 - 2.39 \times T_a)$	Brooker et al. (1992)
k	$(0.0637 + 0.0958 \times M_{ave})/(0.656 - 0.475 \times M_{ave})$	Lague and Jenkins (1991)
M_e	$0.295 - 0.045 \times \ln[-(T + 35.01) \times \ln(RH)]$	ASAE Standards (1999)
ρ_a	1.105	Brooker et al. (1992)
ρ_g	$c_0 \times (1456 + 705 \times M_{ave})$ For hull: $c_0 = 0.532$ For bran: $c_0 = 1.493$ For endosperm: $c_0 = 1.257$	Lague and Jenkins (1991)

[a] where
u = air velocity at kernel surface (m/s)
c_0, c_1, and c_2 = constants.

initial nodal values of temperature and moisture content of a kernel were given, for every time step Δt, a set of new nodal values in the next time step could be calculated. By repeating this procedure, the temperature and moisture fields were obtained.

The thermal and physical properties of rice used in this study and their sources are listed in table 1.

Moisture Content Gradients

In this study, both MCGs and temperature gradients were obtained through finite element simulation. Since it was found in this study that the maximum temperature gradient inside a kernel appeared within 20 s after the onset of drying (refer to fig. 5) and the entire temperature gradients disappeared after 2 to 3 min drying, which coincided with the findings reported by Chen et al. (1999), and owing to the general belief (Sarker et al., 1996; Kunze, 1979; Cnossen and Siebenmorgen, 2000; Yang et al., 2000a) that the main effect of drying on rice milling quality was due to moisture content gradients rather than temperature gradients, focus was placed on reporting moisture content gradients that are defined as:

$$dM/dy \quad (11)$$

where

M = moisture content in % d.b. at any locations inside a rice kernel

y = distance between the location and the center of the kernel.

During the numerical solution, moisture contents were in decimal dry basis. After moisture distribution was obtained, MCGs were reported in % d.b./mm, while moisture contents were converted to percent wet basis to facilitate interpretation and understanding of results. Emphasis was placed on the MCG between the outer bran surface and the kernel center on the short axis of the kernel (i.e., node 2 and node 4 in fig. 1). This was because of two facts: (1) MMCG along the short axis and the maximum temperature gradient along the long axis of a rice kernel were reported by Sarker et al. (1996) and were verified in this study, and (2) brown rice (i.e., everything confined inside the bran surface as demarcated by node 2 and node 6 in fig. 1) is of primary importance because fissures are formed on brown rice despite the existence of the hull. Therefore, the MCGs mentioned later refer to dM/dy between node 2 and node 4.

Experimental Procedures

A long–grain rice variety (Cypress) was harvested at the Rice Research and Extension Center in Stuttgart, Arkansas, in August 1999. It was harvested at intervals during the 1999 season to result in different initial MCs ranging from 16% to 22% w.b. After being cleaned in a Carter–Day Dockage separator (Carter–Day Co., Minneapolis, Minn.), the rice was placed in a sealed plastic barrel and stored at around 4° C until testing. Thin layer drying tests were conducted in the same drying system, as described by Cnossen et al. (1999), at three drying conditions: (1) 42° C drying air temperature, 30% RH, and 16.4% initial moisture content; (2) 60° C drying air temperature, 17% RH, and 21.4% initial moisture content; and (3) 60° C drying air temperature, 17% RH, and 22.1% initial moisture content. The initial rice temperature was around 27° C. The average moisture content at a specific drying duration was measured in triplicate following the same procedure used by Banaszek and Siebenmorgen (1993).

A drill bit of 0.24 mm diameter was used to drill a small hole to the center of a rice kernel. A T–type precision fine–wire thermocouple, 0.254 mm in diameter, was inserted into the hole and glued to immobilize the thermocouple and to prevent drying air from directly contacting the thermocouple tip. One kernel was tested for each drying condition, and three single–kernel temperature profiles were therefore

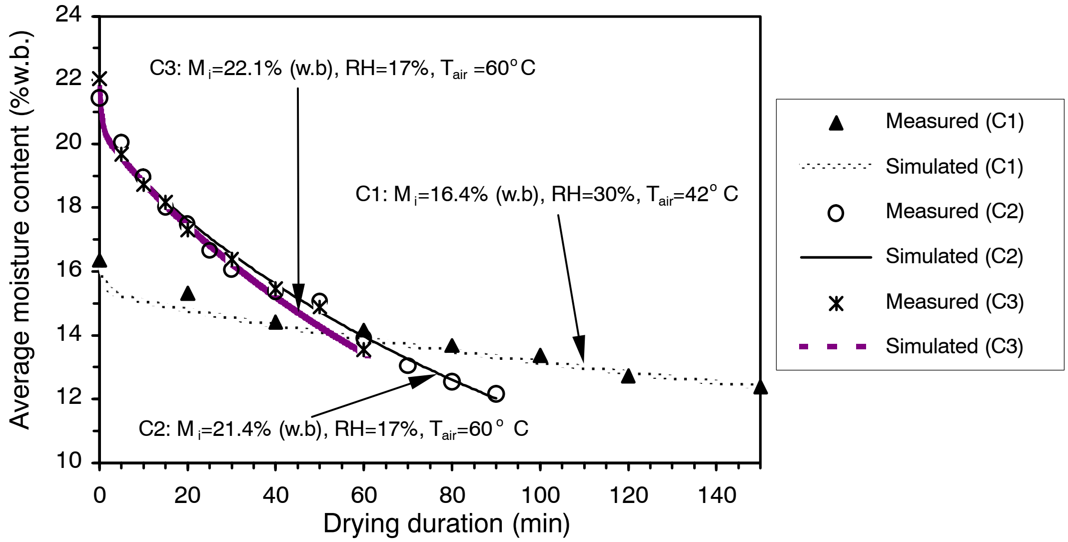

Figure 2. Measured and estimated average moisture contents of rough rice kernels at three thin–layer drying conditions: (C1) 42° C drying air temperature, 30% RH, and 16.4% initial moisture content; (C2) 60° C drying air temperature, 17% RH, and 21.4% initial moisture content; and (C3) 60° C drying air temperature, 17% RH, and 22.1% initial moisture content.

obtained for model verification purpose. To minimize heat conduction into the kernel through the thermocouple, the part of the thermocouple that was exposed to the drying air was insulated with insulation paint. Temperature data were recorded using a Campbell 21X data logger connected to a PC.

Results and Discussion

Drying Simulation and Verification

It is a common practice to verify the drying models by comparing the model–simulated values to the measured mean kernel moisture content and kernel center temperature. In this study, both the model–simulated average moisture content and kernel center temperature compared favorably with the experimentally measured values. Since this article focuses, as mentioned earlier, on reporting moisture responses only, no details are presented on the temperature portion. Figure 2 shows a comparison between the simulated and measured average moisture contents of rice kernels dried at the three different conditions described earlier. As can be seen, the simulated results agreed well with the measured values. This indicates that the finite element model used in this study was capable of predicting temperature and moisture content distributions inside rice kernels.

The estimated moisture content at three locations in the rice kernel (nodes 2, 4, and 6 in fig. 1) is illustrated in figure 3. The moisture content of the kernel center (node 4) did not decrease significantly during the first 20 min of drying. After that, it decreased slowly. The moisture content at node 2 (outer bran along the short axis) decreased very quickly during the first 10 min of drying before it leveled off and approached the equilibrium moisture content of rice. Figure 4 shows the intra–kernel moisture distribution after 15 min and 60 min of drying at 60° C drying temperature and 17% relative humidity. It can be seen that the moisture content at the kernel center was still at a level of about 18% (w.b.) after 60 min of drying. However, the moisture content at the kernel surface quickly approached the equilibrium moisture content of 6% (w.b.) in this drying condition. It is confirmed that the MMCG existed along the short axis, as reported by Sarker et al. (1996). The MCGs between node 4 and node 2 for Cypress reached a maximum value of around 11 (% d.b./mm) in around 28 min, after which it decreased very slowly (fig. 5). In other words, the intra–kernel MCGs remained at a high value throughout the rest of the drying process.

Changes in MCGs have been observed to be closely associated with changes in the milling quality of rice (Sarker et al., 1996; Chen et al., 1999; Yang et al., 2000a, 2000b). Yang et al. (2000a, 2000b) and Fan et al. (2000) reported that a dramatic drop in head rice yield occurred after a certain duration of drying (i.e., after a certain percentage of moisture removal). Yang et al. (2000a, 2000b) found, although more experimental confirmation is needed, that the time when the dramatic drop in head rice yield occurred coincided with the time when the magnitude of MCGs approached its peak value, i.e., in a range of time around the MMCG peak. This can be seen in figure 6, which is redrawn from the data reported by Yang et al. (2000a) for the purpose of illustrating such a relationship.

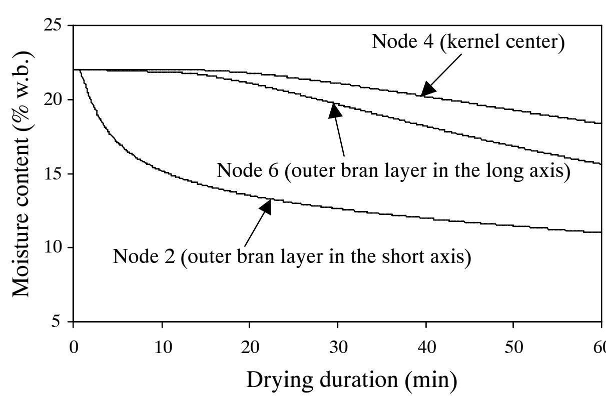

Figure 3. Estimated moisture contents of a rough rice kernel (22.1% w.b. initial moisture content) at three specified nodes at 60° C drying air temperature and 17% air relative humidity.

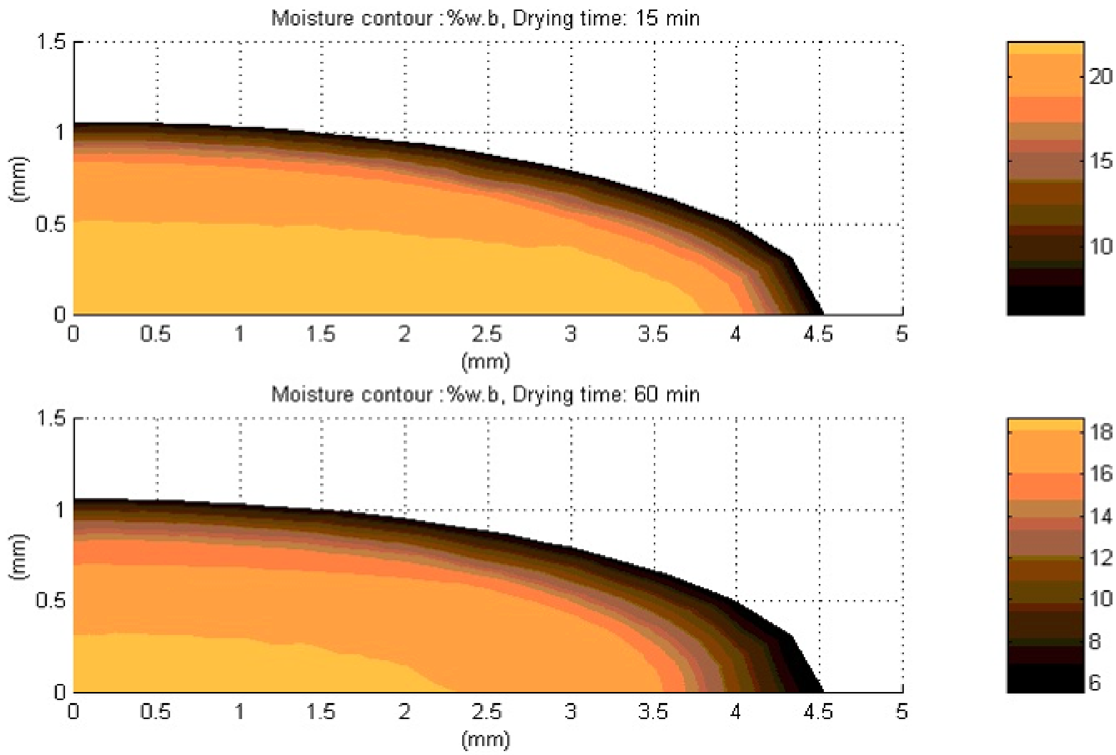

Figure 4. Simulated moisture content distribution inside a rough rice kernel (22.1% w.b. initial moisture content) under 60° C drying air temperature and 17% air relative humidity.

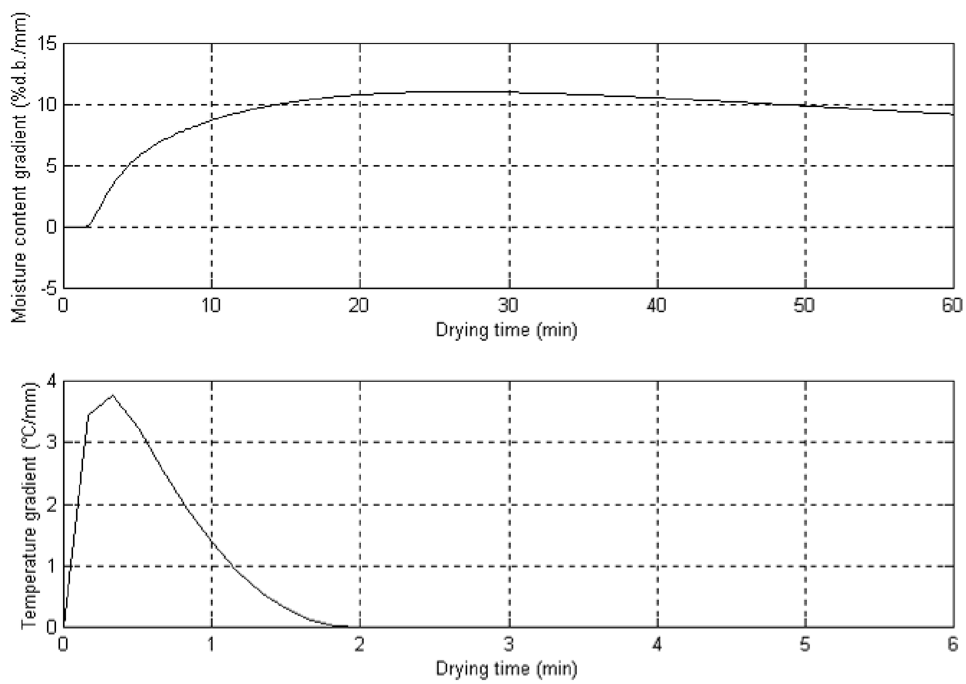

Figure 5. MCGs between node 2 and node 4 and temperature gradients between node 4 and node 6 in figure 1 at 60° C drying air temperature and 17% air relative humidity.

The effect of temperature gradients on the milling quality of rice would generally be minor as compared to that of MCGs. This is because the moisture content of the rice kernels was still high during the first 2 to 3 min of drying, and the drying occurred in the rubbery region (above the Tg curve) where the thermal expansion coefficient was high (Perdon, 1999) and the modulus of elasticity was small. This rendered the kernel rather resilient and not easy to break. On the contrary, as mentioned earlier, the MCG remained at a high value throughout the rest of the drying process after it

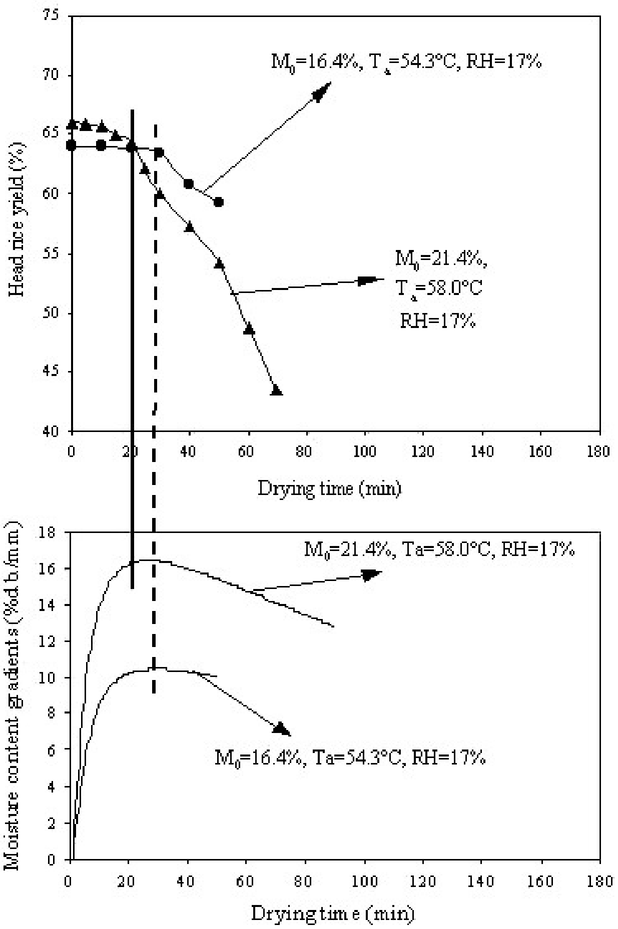

Figure 6. An illustration showing the time when head rice yield started to drop dramatically in the case of no tempering performed on rice after drying coincided with the time around which MCG peaked (redrawn from the data reported by Yang et al., 2000a.)

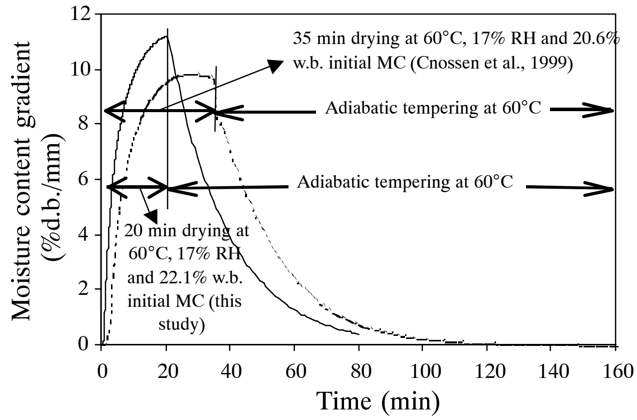

Figure 7. A graph showing the MCGs during drying at 60° C and 17% relative humidity for 20 min and 35 min, respectively, and the subsequent adiabatic tempering at 60° C. The data for 20 min drying were collected in this study with rice at 22.1% w.b. initial moisture content and those for 35 min drying were based on Cnossen et al. (1999) with rice at 20.6% w.b. initial moisture content.

Table 2. Percent MCG reduction due to tempering at selected tempering durations for rice variety Cypress (tempering temperature = 60° C).

Tempering Duration (min)	Percent MCG Reduced Due to Tempering (%)[a] Drying =20 min, 60°C, 17% RH; Initial MC = 22.1% w.b.	Drying = 35 min, 60°C, 17% RH; Initial MC = 20.6% w.b.
10	39	44
20	65	67
30	80	82
40	89	90
50	94	94
60	97	97
80	—	99
95	—	100

[a] Percent MCG reduction = (MCG at the onset of tempering – MCG at a selected tempering duration) / MCG at the onset of tempering × 100.

passed its peak value. Fortes et al. (1981a), Haghighi and Segerlind (1988), and Chen et al. (1999) also reported that a combination of moisture and temperature gradients would produce greater stress levels and fissuring potentials inside the grain kernel. However, the effect of temperature gradients only existed in the very initial stage of drying (about 2 to 3 min). Therefore, the MCGs would have a major effect on stress level of a kernel during the drying process.

Tempering Simulation and Verification

It has been widely recognized that MCGs play an important role in rice fissuring in both absorption and desorption cases (Sarker et al., 1996; Kunze, 1979; Cnossen and Siebenmorgen, 2000; Yang et al., 2000a). Both Fan et al. (2000) and Yang et al. (2000a) reported that when rice was dried in the rubbery region in a glass transition state diagram and cooled down immediately following drying without tempering, head rice yield decreased little until a sufficient MCG built up (i.e., up to a certain percentage of moisture removal). Because MCG remained at a high value throughout the rest of the drying process after it peaked, as can be seen in figure 5, tempering should be used in order to ease a possible contribution of MCGs to hygroscopically induced fissuring. According to figure 5 (upper graph), the MCGs of the Cypress rice kernel reached their maximum in around 28 min at 60° C, 17% relative humidity, and 22.1% (w.b.) initial moisture content. In this study, 20 min of drying, which was slightly before the time when the MMCG was reached, and the subsequent 60 min of tempering were used to simulate the drying and tempering processes.

Figure 7 shows the estimated MCGs during the drying and tempering processes for this case: drying at 60° C, 17% RH, and 22.1% w.b. initial MC for 20 min, followed by adiabatic tempering at 60° C. Figure 7 also shows the MCGs of another case: drying at 60° C, 17% RH, and 20.4% initial MC for 35 min, followed by adiabatic tempering at 60° C, as per Cnossen et al. (1999). In both tempering cases, the intra–kernel MCGs first decreased considerably before they leveled off and gradually approached zero. Table 2 shows the percentage of MCGs for Cypress that was eliminated due to tempering at selected tempering durations based on the MCG data in figure 7. During the first 20 min of tempering, about 67% of the MCGs were removed. With tempering for 40 min, 90% of MCGs diminished. Tempering for 60 min helped eliminate 97% of the MCGs. After 95 min of tempering, all MCGs were eliminated. It is noted that percent MCG reduction followed a similar trend for both cases depicted in figure 7.

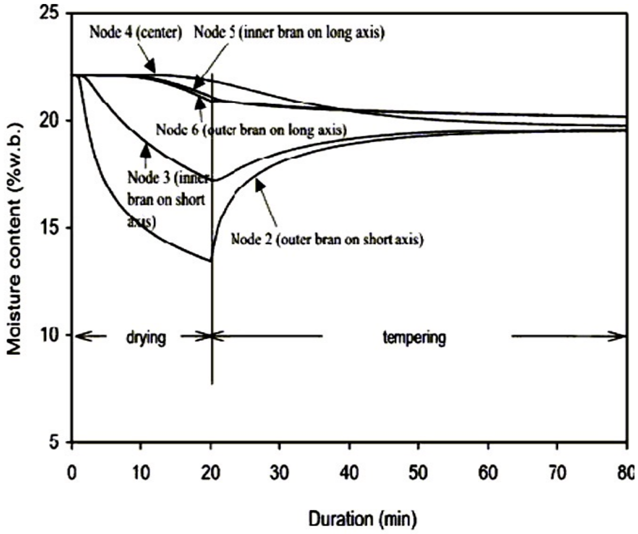

Figure 8. A graph showing the way the estimated moisture content at five specified nodes of a rough rice kernel (22.1% w.b. initial moisture content) changes during the drying and the subsequent adiabatic tempering process. The drying condition was 60° C and 17% relative humidity, and adiabatic tempering was conducted at 60° C.

Figure 8 shows the intra–kernel moisture content responses as the drying and the tempering processes proceeded at node 2 (outer bran on the short axis), node 3 (inner bran on the short axis), node 4 (kernel center), node 5 (inner bran on the long axis), and node 6 (outer bran on the long axis). As can be seen from figure 8, a high MCG was developed between node 2 and node 4 during drying. When tempering was started, the MCG between node 2 and node 4 decreased as the moisture content at node 2 increased and that at node 4 decreased. However, the moisture at node 2 had a much faster and greater change than that at node 4. During tempering, moisture at these nodes would eventually approach the same magnitude. In this simulation, rough rice kernels were first dried for 20 min at 60° C and 17% relative humidity, followed by adiabatic tempering at 60° C. Our simulation results suggested that a tempering time of around 40 min, which accounted for about 90% elimination of MCGs, should theoretically be adequate to alleviate the possible effect of MCGs on head rice reduction. The tempering experiments conducted by Cnossen et al. (1999) corresponded well with the simulation results obtained in this study and indirectly confirmed our results.

Figure 9 shows MCGs during drying at 60° C, 17% RH, and 20.6% (w.b.) initial moisture content and subsequent adiabatic tempering at 60° C. Figure 9 also shows the head rice yields at the endpoint of drying (35 min) and six tempering durations at 40–min intervals, as reported by Cnossen et al. (1999). At the end of drying, head rice yield dropped to 58.9% (without tempering) from the level of the control sample (64.5%). However, when rice was tempered at 60° C for 40 min immediately after drying, where 90% MCGs were eliminated as mentioned earlier, head rice yield recovered completely (65%) and stayed fairly constant throughout the rest of the tempering duration at 40–min intervals.

The significance of this study is that a theoretically optimal tempering duration in which HRY reduction is minimal could be established in terms of 90% reduction in moisture content gradients through finite element simulation.

Summary and Conclusions

Finite element models were used to simulate the single kernel drying and tempering behavior of rice in terms of moisture and temperature distributions inside rice kernels. Maximum moisture content gradients existed along the short axis of a rice kernel. The intra–kernel moisture content gradients decreased considerably during the first 40 min of tempering, after which they decreased slowly and approached zero. During tempering, the moisture content at the kernel surface increased and that at the kernel center decreased to finally reach a uniform moisture content in all parts of the kernel when sufficient tempering time was allowed. According to the finite element simulation, 40 min of tempering at 60° C for rice with 20.4% initial moisture content that was dried up to 35 min at 60° C and 17% relative

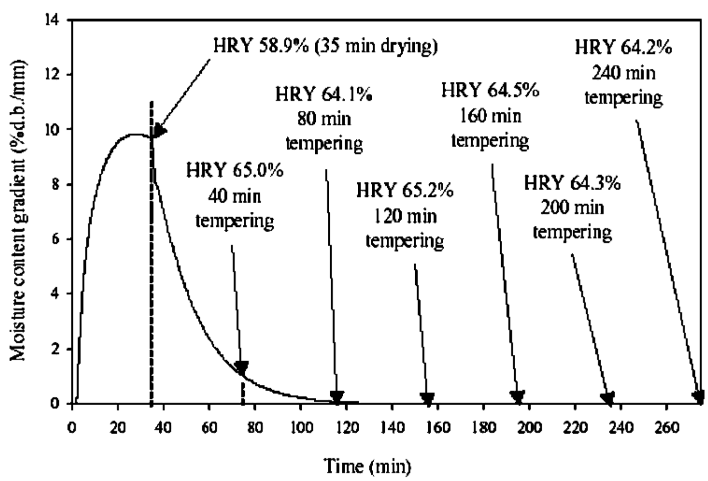

Figure 9. A graph showing the MCGs at 60° C drying air temperature, 17% air relative humidity, and 20.6% w.b. initial moisture content, as well as the head rice yields at the end of drying and at the six tempering durations. Data were based on Cnossen et al. (1999). The head rice yield of the control sample was 64.5%.

humidity was able to eliminate a majority (i.e., around 90%) of the MCGs created during drying, thus preserving the head rice yield. This simulation result corresponded well with the experimental data of Cnossen et al. (1999).

References

ASAE Standards, 46th ed. 1999. D245.5: Moisture relationships of plant–based agricultural products. St. Joseph, Mich.: ASAE.

Banaszek, M. M., and J. T. Siebenmorgen. 1993. Individual rice kernel drying curves. *Trans. ASAE* 36(2): 521–527.

Bautista, R. C., T. J. Siebenmorgen, and A. G. Cnossen. 2000. Characteristics of rice individual kernel moisture content and size distributions at harvest and during drying. Paper No. 325. In *Proc. 12th International Drying Symposium IDS2000*. Noordwijkerhout, The Netherlands. Amsterdam, The Netherlands: Elsevier Science.

Brooker, D. B., F. W. Bakker–Arkema, and C. W. Hall. 1992. *Drying and Storage of Grains and Oilseeds*. New York, N.Y.: Van Nostrand Reinhold.

Chen, H., T. J. Siebenmorgen, and W. Yang. 1999. Finite element simulation to relate head rice yield reduction during drying to internal kernel moisture gradient and rice state transition. ASAE Paper No. 996156. St. Joseph, Mich.: ASAE.

Cnossen, A. G., and T. J. Siebenmorgen. 2000. The glass transition temperature concept in rice drying and tempering: Effect on milling quality. *Trans. ASAE* 43(6): 1661–1667.

Cnossen, A. G., T. J. Siebenmorgen, J. D. Reid, and W. Yang. 1999. Incorporating the glass transition temperature concept in rice drying and tempering to optimize moisture removal and milling quality. ASAE Paper No. 996022. St. Joseph, Mich.: ASAE.

Fan, J., T. J. Siebenmorgen, and W. Yang. 2000. A study of head rice yield reduction of long– and medium–grain rice varieties in relation to various harvest and drying conditions. *Trans. ASAE* 43(6): 1709–1714.

Fortes, M., M. R. Okos, and J. R. Barrett. 1981a. Heat and mass transfer analysis of intra–kernel wheat drying and rewetting. *J. Agric. Eng. Research* 26(1): 109–112.

_____. 1981b. Non–equilibrium thermodynamics approach to heat and mass transfer in corn kernels. *Trans. ASAE* 24(3): 761–769.

Gustafson, R. J., A. Y. Mahmoud, and G. E. Hall. 1983. Breakage susceptibility reduction by short–term tempering of corn. *Trans. ASAE* 26(3): 918–922.

Haghighi, K., and L. J. Segerlind. 1988. Modeling simultaneous heat and mass transfer in an isotropic sphere: A finite element approach. *Trans. ASAE* 31(2): 629–637.

Haghighi, K., J. Irudayaraj, R. L. Stroshine, and S. Sokhansanj. 1990. Grain kernel drying simulation using the finite element method. *Trans. ASAE* 33(6): 1957–1965.

Husain A., C. S. Chen, J. T. Clayton, and L. F. Whitney. 1972. Mathematical simulation of heat and mass transfer in high–moisture foods. *Trans. ASAE* 15(3): 732–736.

Husain A., C. S. Chen, and J. T. Clayton. 1973. Simultaneous heat and mass diffusion in biological materials. *J. Agric. Eng. Research* 18(3): 343–354.

Irudayaraj, J., K. Haghighi, and R. L. Stroshine. 1992. Finite element analysis of drying with application to cereal grains. *J. Agric. Eng. Research* 53(2): 209–229.

Jia, C.–C., Y. B. Li, D. Y. Liu, and C. W. Cao. 1996. Mathematical simulation of the moisture content distribution within a corn kernel during tempering. *Trans. Chinese Society of Agric. Eng.* 12(1): 147–151.

Jia, C.–C., D. Sun, and C. W. Cao. 2000. Mathematical simulation of temperature and moisture fields within a grain kernel during drying. *Drying Technology* 18(6): 1305–1325.

Kunze, O. R. 1979. Fissuring of the rice grain after heated air drying. *Trans. ASAE* 22(5): 1197–1201, 1207.

Lague, L., and B. M. Jenkins. 1991. Modeling pre–harvest stress–cracking of rice kernels: Part 2. Implementation and use of the model. *Trans. ASAE* 34(4): 1812–1823.

Luikov, A. V. 1966. *Heat and Mass Transfer in Capillary Bodies*. New York, N.Y.: Pergamon Press.

Perdon, A. A. 1999. Amorphous state transition in rice during the drying process. PhD diss. Fayetteville, Ark.: University of Arkansas.

Sarker, N. N., O. R. Kunze, and T. Strouboulis. 1996. Transient moisture gradients in rough rice mapped with finite element model and related to fissures after heated air drying. *Trans. ASAE* 39(2): 625–631.

Sokhansanj, S., and D. M. Bruce. 1987. A conduction model to predict grain drying simulation. *Trans. ASAE* 30(4): 1181–1184.

Steffe, J. F., and R. P. Singh. 1980a. Liquid diffusivity of rough rice components. *Trans. ASAE* 23(3): 767–774.

_____. 1980b. Theoretical and practical aspects of rough rice tempering. *Trans. ASAE* 23(3): 775–782.

Wasserman, T., R. E. Ferrel, D. F. Houston, E. Breitweiser, and G. S. Smith. 1964. Tempering western rice. *Rice J.* 67(2): 16, 17, 20–22.

Yang, W., C.–C. Jia, T. J. Siebenmorgen, and A. G. Cnossen. 2000a. Intra–kernel moisture gradients and glass transition temperature in relation to head rice yield variation during heated air drying of rough rice. Paper No. 069. In *Proc. 12th International Drying Symposium IDS2000*. Noordwijkerhout, The Netherlands. Amsterdam, The Netherlands: Elsevier Science.

Yang, W., T. J. Siebenmorgen, C.–C. Jia, T. A. Howell, and A. G. Cnossen. 2000b. Cross–flow drying of rough rice as mapped on its glass transition state diagram. Paper No. 068. In *Proc. 12th International Drying Symposium IDS2000*. Noordwijkerhout, The Netherlands. Amsterdam, The Netherlands: Elsevier Science.

Nomenclature

A = surface area of a grain kernel (m^2)
c = specific heat (J/kg °C)
D = effective overall moisture diffusion coefficient (m^2/h)
h_m = convective mass transfer coefficient (m/s)
h_t = convective heat transfer coefficient (W/m^2 °C)
k = thermal conductivity of a single grain kernel (W/m °C)
M = moisture content of a single grain kernel (d.b.; dry basis used in simulation and converted to wet basis at the end)
n = gradient normal to kernel surface
Q_{fg} = latent heat of vaporization (J/kg)
t = drying time (s)
T = temperature of a single grain kernel (°C)
V = volume of a grain kernel (m^3)

Greek symbols

ρ = density of a single grain kernel (kg/m^3)

Subscripts

0 = initial
a = drying air
ave = average
e = equilibrium
g = grain
v = water vapor